Graphene-MoS2 hybrid nanostructures enhanced surface plasmon resonance biosensors

Zeng, Shuwen; Hu, Siyi; Xia, Jing; Anderson, Tommy; Dinh, Xuan-Quyen; Meng, Xiang-Min; Coquet, Philippe; Yong, Ken-Tye

2014

Zeng, S., Hu, S., Xia, J., Anderson, T., Dinh, X.-Q., Meng, X.-M., et al. (2015). Graphene-MoS2 hybrid nanostructures enhanced surface plasmon resonance biosensors. Sensors and Actuators B : chemical, 207, 801–810.

https://hdl.handle.net/10356/103773

https://doi.org/10.1016/j.snb.2014.10.124

Graphene–MoS_2 Hybrid Nanostructures enhanced Surface Plasmon Resonance Biosensors

Shuwen Zeng[1,2], Siyi Hu[2,4], Jing Xia[3], Tommy Anderson[2], Xuan-Quyen Dinh[1], Xiang-Min Meng[3], Philippe Coquet[1,5] and Ken-Tye Yong[1,2*]

[1]CINTRA CNRS/NTU/THALES, UMI 3288, Research Techno Plaza, 50 Nanyang Drive, Border X Block, Singapore, 637553

[2]School of Electrical and Electronic Engineering, Nanyang Technological University, Singapore, 639798

E-mail: ktyong@ntu.edu.sg, Tel.: +65 67905444

[3]Key Laboratory of Photochemical Conversion and Optoelectronic Materials, Technical Institute of Physics and Chemistry, Chinese Academy of Sciences, Beijing, P.R. China

[4]School of Science, Changchun University of Science and Technology, Changchun 130022, Jilin, China

[5]Institut d'Electronique, de Microélectronique et de Nanotechnologie (IEMN), CNRS UMR 8520 – Université de Lille 1, 59650 Villeneuve d'Ascq, France

Abstract

In this work, we propose a new configuration of surface plasmon resonance (SPR) sensor that is based on graphene-MoS_2 hybrid structures for ultrasensitive detection of molecules. The proposed system displays a phase-sensitivity enhancement factor of more than 500-fold when compared to the SPR sensing scheme without the graphene-MoS_2 coating or with only graphene coating. Our hypothesis is that the monolayer MoS_2 has a much higher optical absorption efficiency (~5%) than that of the graphene layer (~2.3%). Based on our findings, the electron energy loss of MoS_2 layer is comparable to that of graphene and this will allow a successful (~100%) of light energy transfer to the graphene-MoS_2 coated sensing substrate. Such process will lead to a significant enhancement of SPR signals. Our simulation shows that a quasi-dark point of the reflected light can be achieved under this condition and this has resulted in a steep phase jump at the resonance angle of our newly proposed SPR system. More importantly, we found that phase interrogation detection approach of the graphene-MoS_2 hybrid structures-based sensing system is more sensitive than that of using the regularly angular interrogation method and our theoretical analysis indicates that 45 nm of Au film thickness and 3 coating layers of MoS_2 nanosheet are the optimized parameters needed for the proposed SPR system to achieve the highest detection sensitivity range.

1. Introduction

Two-dimensional (2D) nanomaterials have received great attention from the nanotechnology community in recent years due to their potential applications ranging from transistors to photodetectors [1-10]. For example, graphene is one of the most extensively studied 2D nanomaterial to date since its first discovery in 2004 [11]. It is considered as the thinnest man-made material (~0.34 nm) that is only composed of a single layer of hexagonally arranged carbon atoms and it is also known as the one of the strongest materials with a high breaking strength of 42 N/m which is at least 2 orders of magnitude stronger than that of the common steel. This unique intrinsic mechanical property makes graphene a promising 2D nanomaterial for cost-effective fabrication of high-quality sensing substrates and display screens. Although graphene is known as the building block for a wide range of carbon materials such as 0D fullerene, 1D carbon nanotubes (CNTs) and 3D bulk graphite, its electronic and optical properties are significantly different when compared to allotropes mentioned above. For instance, the charge carrier mobility of graphene is reported to be as high as 10^6 cm^2 V^{-1} s^{-1} [12]. Thus, when graphene layers are deposited on metallic thin films or functionalized with metallic nanoparticles (e.g., Au or Ag), strong coupling can be induced at the metallic/graphene interface due to the effective charge transfer and this generates a large electric field enhancement at the nano-interface [13-18]. The electric field excited on the metallic surface is an evanescent wave and is sensitive towards the refractive-index change of its surrounding media. This phenomenon is generally referred as surface plasmon resonance (SPR). SPR sensors are the commonly used optical sensors for real-time monitoring of various biomolecular interactions such as DNA hybridization and protein bindings [2, 19-21]. Recent studies have shown that graphene can be used as an enhanced SPR substrate for biosensing applications. There are several advantages for using graphene-based SPR substrate for sensing: i) they are able to induce significantly large field enhancement at the substrate interface; ii) graphene has relatively large surface area (~2630 m^2 g^{-1}) thus allowing it to have a better surface contact with the analyte; and iii) graphene surface can selectively detect aromatic compounds through pi-stacking force and this will help one to be able to study challenging experiments such as DNA interaction with proteins at extreme dilute condition [22-24]. However, it was reported that graphene-based SPR sensors possessed the highest detection sensitivity when the total number of graphene layers deposited on the metallic SPR sensing substrate (50 nm) is larger than 10. Even with such thick layers of graphene on the

SPR substrate, the sensitivity enhancement factor has only increased from 1.25 to 2, which is considered to be an incremental improvement for the sensitivity of the SPR biosensor [22, 25-28]. This incremental enhancement factor is mainly attributed to: i) the angular-interrogation measurement method is generally used in these reported experiments where the change of resonance angle with the index perturbation on the sensing surface is proportional to the thickness of the high-refractive-index dielectric layer coated onto the Au thin film; and ii) the low optical absorption (~2.3%) of graphene [29, 30] is not able to absorb sufficient energy to promote the excitation process of an efficient charge transfer between graphene and the metallic thin film. It is also worth noting that one can increase the thickness of metallic thin film to reduce the needed number of graphene layers (e.g., 60 nm silver thin film coated with monolayer graphene) [25] for sensing, but this will result in a much higher fabrication cost for preparing the SPR sensing substrate. Thus, this indicates that new alternative SPR sensing substrates must be developed to further push the envelope of the sensitivity of the SPR system.

More recently, ultra-thin layer of molybdenum disulfide (MoS_2) that belongs to the transition-metal dichalcogenide (TMDC) semiconductor group is known as "beyond graphene" 2D nanocrystals material [31-33] and they are widely used as solid lubricants due to its low friction property. These 2D crystals composed of two-dimensional layers stacked in the vertical direction via van der Waals force. Similar to graphene, monolayer MoS_2 can be prepared by micromechanical cleavage or synthesized using chemical vapor deposition (CVD) method [8, 34]. When the thickness of MoS_2 crystal is thinned down to monolayer (~0.65nm), a new set of electronic and optical property can be obtained. For example, bulk MoS_2 has an indirect bandgap of 1.2 eV while monolayer MoS_2 has a direct bandgap of 1.8 eV due to quantum confinement effects [35, 36]. This unique feature allows MoS_2 to serve as the nano-transistor channel with larger switching on/off ratios [8, 33]. Also, monolayer of MoS_2 possessed a high optical absorption efficiency (~5%) that can be utilized to fabricate ultrasensitive photodetectors with a responsivity up to 5×10^8 A W^{-1} [34, 36-38]. Based on these unique features of MoS_2 nanosheets, we proposed and designed a new configuration of enhanced SPR biosensors that is based on graphene-MoS_2 hybrid structures as shown in Fig. 1. The designed SPR sensing substrate consists of Au thin film and the film is coated with MoS_2 nanosheets and monolayer graphene. Since the work function of Au (5.54 eV) is higher than that of MoS_2 and graphene (5.1 eV and 4.5 eV), successful transfer of electrons from MoS_2/graphene hybrid layers to Au film will occur

under optical excitation [39-41]. This process will lead to a larger electric field enhancement at the sensing interface thereby resulting in a higher sensitivity to the target analytes [2]. In our proposed system, MoS_2 layers are used for improving the light absorption in order to provide enough excitation energy for effective charge transfer, while monolayer graphene is acting as bio-recognition component for capturing the target biomolecules through pi-stacking force. In this study, the SPR sensing performance is systematically investigated by varying the thickness of Au thin film and number of MoS_2 layers using transfer-matrix analysis. Since the Heaviside step-like phase changes are much sharper than the resonance angle shift, the sensitivity enhancement of our proposed system can be significantly improved. In our theoretical analysis, we show that the sharpest phase signal change and lowest value of minimum reflectivity can be achieved when SPR substrate of 45 nm Au thin film coated by 3 layers of MoS_2 and 1 monolayer of graphene is used. The phase sensitivity of this system is increased by more than 2 orders when compared to those sensing substrate with "naked" Au thin film or Au thin film coated with graphene.

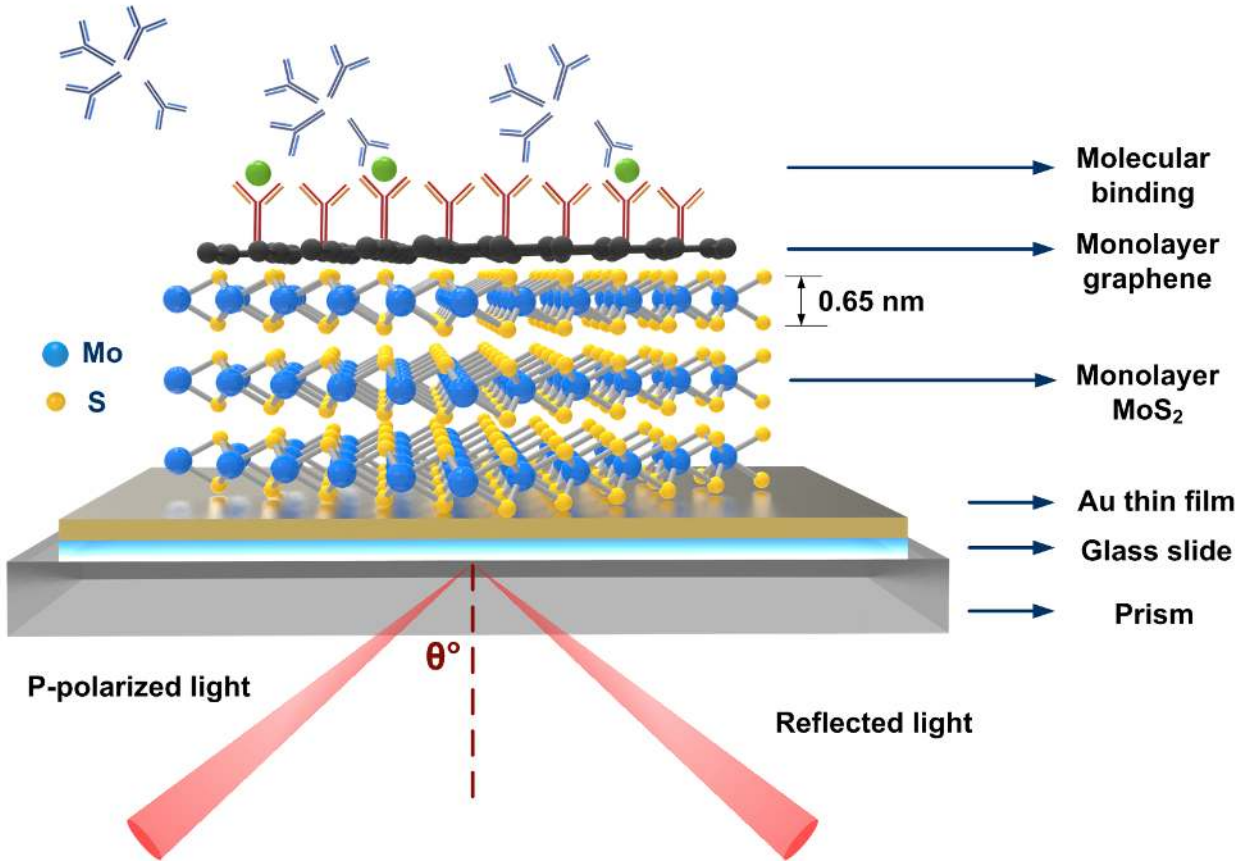

Fig. 1. Schematic diagram of graphene-MoS_2 enhanced SPR biosensor.

2. Design consideration and theoretical model

In our proposed new configuration, a well-known Kretschmann configuration is employed [20], where the Au thin film coated glass slide is attached to the base of an equilateral prism made of high refractive index glass through index matching fluid. Before the attachment to prism, graphene and MoS_2 layers are deposited on the top of the Au thin film coated glass slide [9, 42, 43]. The excitation light wavelength used for the SPR sensing is 632.8 nm. The TM-polarized light is incident from one lateral face of the prism, then reached to its base and totally reflected out from the other lateral face and collected and analyzed by a photodetector.

2.1. Refractive index of various layer components

The first layer is the SF11 prism and its refractive index (n_1) is calculated through the following relation [44]:

$$n_1 = \left(\frac{1.73759695\lambda^2}{\lambda^2 - 0.013188707} + \frac{0.313747346\lambda^2}{\lambda^2 - 0.0623068142} + \frac{1.89878101\lambda^2}{\lambda^2 - 155.23629} + 1 \right)^{1/2} \quad (1)$$

where λ is the wavelength of incident light in μm. Eq. (1) is valid for wavelengths ranging from 0.37 to 2.50 μm. Similarly, the second layer is the BK7 glass slide and its refractive index (n_2) is determined by the following relation [44]:

$$n_2 = \left(\frac{1.03961212\lambda^2}{\lambda^2 - 0.00600069867} + \frac{0.231792344\lambda^2}{\lambda^2 - 0.0200179144} + \frac{1.01046945\lambda^2}{\lambda^2 - 103.560653} + 1 \right)^{1/2} \quad (2)$$

where λ is the wavelength of incident light in μm. Eq. (2) is valid for wavelengths ranging from 0.30 to 2.50 μm. The complex refractive index of titanium adhesion layer (n_3) at 632.8 nm is obtained from the experimental measurement data by Palik [45]. The fourth layer is the Au thin film and its complex refractive index (n_4) is calculated through the Drude model as follow [46, 47]:

$$n_4 = \left(\varepsilon_{4r} + i\varepsilon_{4i} \right)^{1/2} = \left(1 - \frac{\lambda^2 \lambda_c}{\lambda_p^2 (\lambda_c + i\lambda)} \right)^{1/2} \quad (3)$$

where λ_p (1.6826 × 10^{-7} m) and λ_c (8.9342 × 10^{-6} m) represent the plasma and the collision wavelengths of gold, respectively. The complex refractive index of monolayer MoS_2 (n_5) at 632.8 nm is obtained from the experimental measurement data by Castellanos-Gomez et al [48] and the thickness of MoS_2 layers (d_5) = L × 0.65 nm [35], where L is the number of MoS_2 layer. The sixth layer of our model is monolayer graphene (d_6 = 0.34 nm) and its complex refractive index (n_6) in the visible range is give as [49]:

$$n_6 = 3.0 + i\frac{C_1}{3}\lambda \tag{4}$$

where the constant $C_1 \approx 5.446$ μm^{-1} [29] and λ is the wavelength of incident light in μm. The sensing medium for initial calibration is deionized (DI) water and its refractive index (n_7) is determined by the following relation [50]:

$$n_7^2 - 1 = \sum_{i=1}^{4} \frac{A_i \lambda^2}{\lambda^2 - t_i^2} \tag{5}$$

where the Sellmeier coefficients A_1 = 5.666959820 × 10^{-1}, A_2 = 1.731900098 × 10^{-1}, A_3 = 2.095951857 × 10^{-2}, A_4 = 1.125228406 × 10^{-1}, t_1 = 5.084151894 × 10^{-3}, t_2 = 1.818488474 × 10^{-2}, t_3 = 2.625439472 × 10^{-2}, t_4 = 1.073842352 × 10^{1} and λ is the wavelength of incident light in μm. Eq. (5) is valid for wavelengths ranging from 0.182 to 1.129 μm. The refractive-index change of the sensing medium induced by the adsorption of biomolecules on the surface of monolayer graphene is denoted by Δn_{bio}. Thus, based on the above parameters and equations, the refractive indices of the seven layers used in our SPR modeling at 632.8 nm are respectively: n_1 = 1.7786, n_2 = 1.5151, n_3 = 2.1526 + i2.9241, n_4 = 0.1838 + i3.4313, n_5 = 5.9000 + i0.8000, n_6 = 3.0000 + i1.1487, n_7 = 1.3320 + Δn_{bio}.

2.2. Phase (ϕ_p) and reflectivity (R_p)

To systematically investigate the phase and reflectivity change in our graphene-MoS_2 hybrid structure based SPR sensing system, we employed the transfer matrix method (TMM) and Fresnel equations based on an N-layer model to perform a detailed analysis. The layers are parallelly stacked along in the Z-direction that is perpendicular to the sensing interface and each layer is defined by their respective dielectric constant ($\varepsilon = n^2$) and thickness (d). All layers are set

to be optically isotropic and non-magnetic. The electromagnetic fields at the first boundary Z_1 in the tangential direction is set as $Z = Z_1 = 0$. And the relation of the tangential fields of the last boundary Z_{N-1} and the first boundary Z_1 is given as [22, 46]:

$$\begin{bmatrix} U_1 \\ V_1 \end{bmatrix} = M \begin{bmatrix} U_{N-1} \\ V_{N-1} \end{bmatrix} \tag{6}$$

where U_1 and U_{N-1} are respectively the tangential component of electric field at the boundary of the first layer and the Nth layer, V_1 and V_{N-1} are respectively the tangential component of magnetic field at the boundary of the first layer and the Nth layer, M is known as the characteristic Transfer Matrix (TM) of the combined N-layer structure and can be obtained through the following relation for the p-polarization light [51, 52]:

$$M = \prod_{k=2}^{N-1} M_k = \begin{bmatrix} M_{11} & M_{12} \\ M_{21} & M_{22} \end{bmatrix} \tag{7}$$

with

$$M_k = \begin{bmatrix} \cos\beta_k & (-i\sin\beta_k)/q_k \\ -iq_k \sin\beta_k & \cos\beta_k \end{bmatrix} \tag{8}$$

where

$$q_k = \left(\frac{\mu_k}{\varepsilon_k} \right)^{1/2} \cos\theta_k = \frac{(\varepsilon_k - n_1^2 \sin^2\theta_1)^{1/2}}{\varepsilon_k} \tag{9}$$

and

$$\beta_k = \frac{2\pi}{\lambda} n_k \cos\theta_k (z_k - z_{k-1}) = \frac{2\pi d_k}{\lambda} (\varepsilon_k - n_1^2 \sin^2\theta_1)^{1/2} \tag{10}$$

Here, ε_k and d_k represent the dielectric constant and thickness of the k-th layer, θ_1 and λ are respectively the incident angle and wavelength at the base of SF11 prism as shown in Fig. 1. The total reflection coefficient (r_p) for the p-polarization light is related to the matrix as follows:

$$r_p = \frac{(M_{11} + M_{12} q_N) q_1 - (M_{21} + M_{22} q_N)}{(M_{11} + M_{12} q_N) q_1 + (M_{21} + M_{22} q_N)} \tag{11}$$

where q_1 and q_N are the corresponding terms for the first layer (SF11 prism) and N-th layer (the sensing medium that contains the target biomolecules) from Eq. (9). Finally, the phase (ϕ_p) and reflectivity (R_p) of the p-polarization light are obtained as:

$$\phi_p = \arg\left(r_p\right) \tag{12}$$

and

$$R_p = \left|r_p\right|^2 \tag{13}$$

For s-polarization light the above equations hold except:

$$q_k = \left(\frac{\varepsilon_k}{\mu_k}\right)^{1/2} \cos\theta_k = \left(\varepsilon_k - n_1^2 \sin^2\theta_1\right)^{1/2} \tag{14}$$

It is known that SPR only affects p-polarization light (i.e., transverse magnetic waves), therefore s-polarization light (i.e., transverse electric waves) can be served as a reference signal to eliminate environmental noises for improving the stability and accuracy of SPR sensors throughout the measurement [20, 47]. The differential phase between p- and s- polarization is obtained as $\phi_d = |\phi_p - \phi_s|$.

The plot of reflectivity (R_p) versus incident angle (θ_{inc}) is called SPR curve, where the resonant dip angle (θ_{SPR}) corresponds to the minimum value of the reflectivity and changes with the refractive-index change Δn_{bio} of the sensing medium that is induced by the binding of the target biomolecules. The shift of the resonance angle is due to the wave vector matching (i.e., the SPR excitation condition) between the incident light along the direction of SP propagation (k_x) and the surface plasmon waves (k_{SP}) as follows:

$$k_x = k_{SP} \quad \text{with } k_x = k_0 n_{prism} \sin\theta_{SPR} \text{ and } k_{SP} = \mathrm{Re}\left[k_0 \left(\frac{\varepsilon_{mmg} n_s^2}{\varepsilon_{mmg} + n_s^2}\right)^{1/2}\right] \tag{15}$$

where k_0 is the wave vector of the incident light in free space, ε_{mmg} is the dielectric constant of the graphene-MoS_2 enhanced metallic thin film and n_s is the refractive index of the sensing medium that contains target biomolecules. It is worth noting that an abrupt phase change would occur at the resonant

dip angle (θ_{SPR}) where the reflected light intensity is approaching zero (i.e., a point of quasi-darkness). The darker the reflectivity, the sharper the phase jump [53]. Thus, even a tiny refractive-index change that is induced by the flow in of target biomolecules solutions (1 nM to 1 pM) can be detected by the sharp phase signal ($\Delta\phi_d$) measured at a fixed θ_{SPR} corresponding to the initial calibration sensing medium. The SPR phase sensitivity (S_p) is defined by:

$$S_p = \frac{\Delta\phi_d}{\Delta n_{bio}} \tag{16}$$

The enhancement factor (E_p) of phase sensitivity with graphene-MoS_2 enhanced metallic thin film (S_{pmmg}) against that of the pure metallic thin film (S_{pm}) is given as:

$$E_p = \frac{S_{pmmg}}{S_{pm}} = \frac{\Delta\phi_{dmmg} / \Delta n_{bio}}{\Delta\phi_{dm} / \Delta n_{bio}} = \frac{\Delta\phi_{dmmg}}{\Delta\phi_{dm}} \tag{17}$$

where $\Delta\phi_{dmmg}$ and $\Delta\phi_{dm}$ are respectively the differential phase changes corresponding to Δn_{bio} with the graphene-MoS_2 enhanced metallic thin film and the pure metallic thin film.

3. Results and discussion

From Eq. (16) and Eq. (17), one can see that the SPR phase sensitivity (S_p) and enhancement factor (E_p) of graphene-MoS_2 coated metallic thin film sensing substrate are essentially determined by the differential phase change ($\Delta\phi_d$) for a fixed refractive index variation (Δn_{bio}) induced by the molecular interaction on the sensing surface. The sharpest phase change of *p*-polarization light under SPR excitation condition only occurs at the point where the intensity of the reflected light is at the minimum that is close to zero [53, 54]. Since there is a trade-off between the enhancement effect and the electron energy loss by inserting MoS_2 layers between monolayer graphene and Au thin film for achieving the minimum reflectivity, we first systematically investigated the effects of Au thickness and number of MoS_2 layer on the spectral reflectivity and phase of SPR curves and this can be achieved by using Eq. (12) and Eq. (13). The refractive index of sensing medium is fixed at 1.332 that is corresponded to DI water.

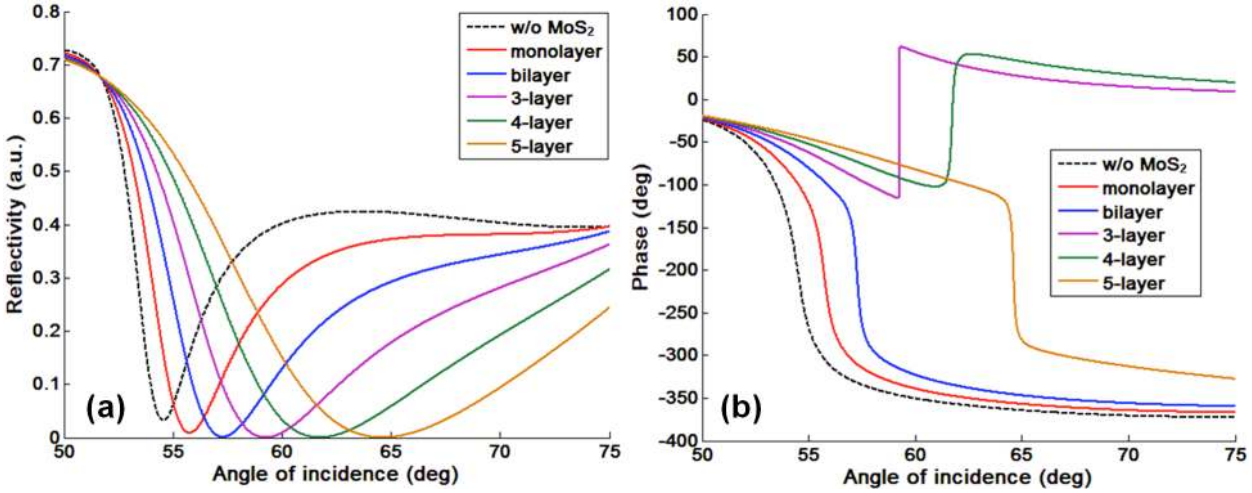

Fig. 2. Variation of (a) reflectivity and (b) phase with respect to angle of incidence for different number of MoS_2 layers with sensing layer refractive index 1.332 at wavelength 632.8 nm. The thickness of the gold layer is 45 nm.

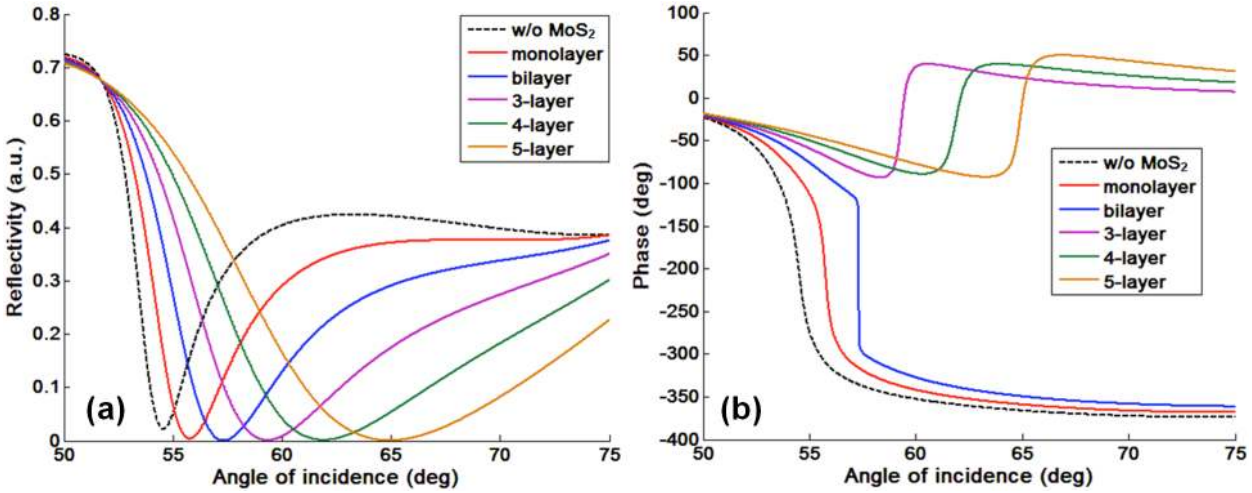

Fig. 3. Variation of (a) reflectivity and (b) phase with respect to angle of incidence for different number of MoS_2 layers with sensing layer refractive index 1.332 at wavelength 632.8 nm. The thickness of the gold layer is 46 nm.

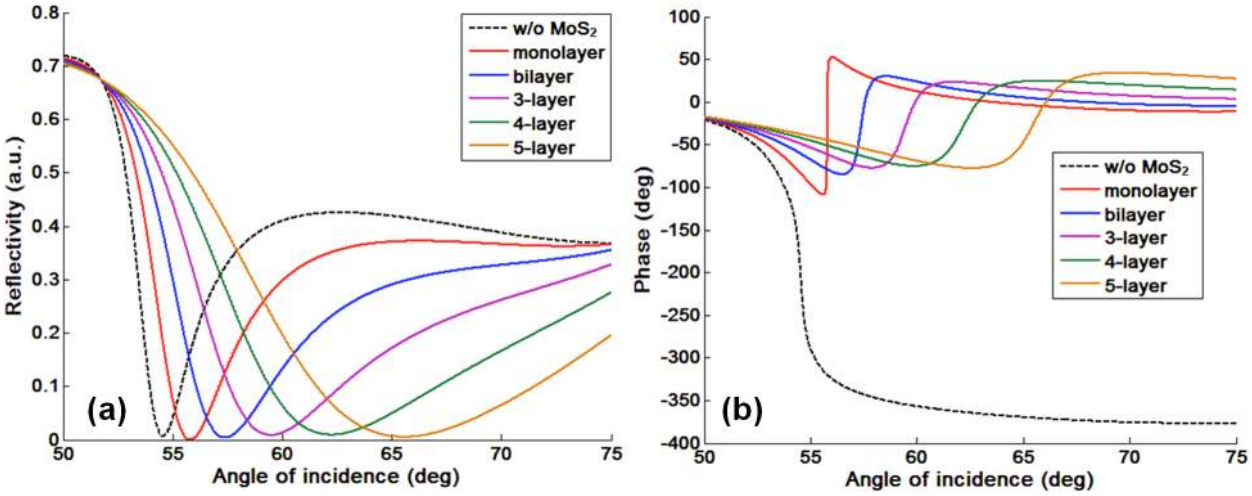

Fig. 4. Variation of (a) reflectivity and (b) phase with respect to angle of incidence for different number of MoS_2 layers with sensing layer refractive index 1.332 at wavelength 632.8 nm. The thickness of the gold layer is 48 nm.

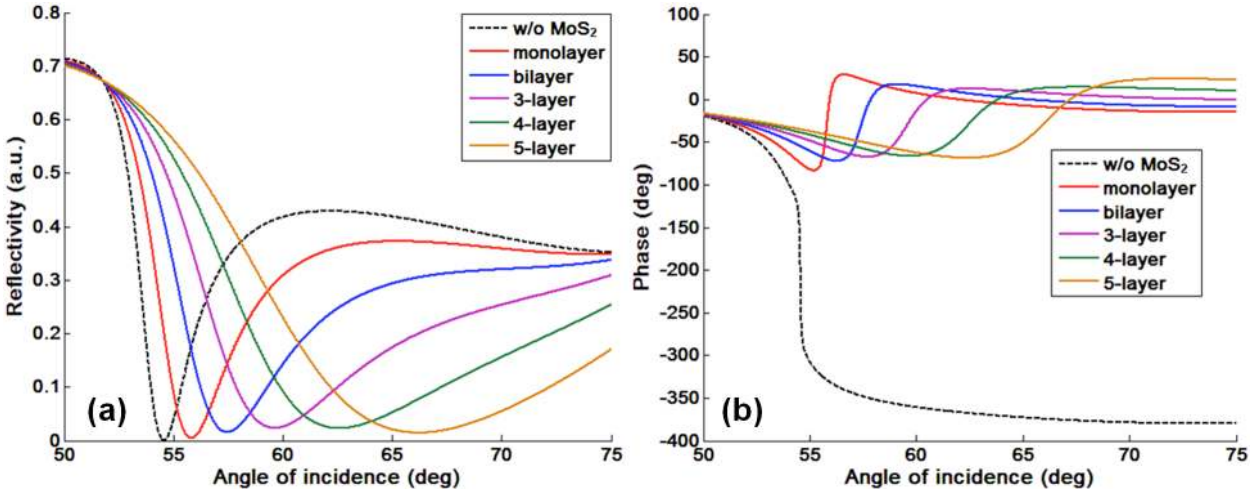

Fig. 5. Variation of (a) reflectivity and (b) phase with respect to angle of incidence for different number of MoS_2 layers with sensing layer refractive index 1.332 at wavelength 632.8 nm. The thickness of the gold layer is 50 nm.

There are three important features that can be observed from the graphene-MoS_2 SPR reflectivity curves (Fig. 2a-5a, Fig. S1a-S12a and Supplementary Video 1): (i) The SPR resonance angle (θ_{SPR}) has a large red shift with increasing number of MoS_2 layers at a fixed Au thin film

thickness that is due to the large value of the real part of the MoS_2 dielectric function. According to the excitation condition in Eq. (15), increasing the real part of the MoS_2 dielectric function will lead to an increase of the SP wavevector (k_{SP}) (i.e., a decrease of the SP propagation velocity) [55]. As a result, a larger incident angle is required for the excitation of SPR; (ii) A rapid broadening of the curves is observed when the number of MoS_2 layers deposited on the Au thin film increases and this is caused by the electron energy loss of MoS_2 layers which is related to the imaginary part of their dielectric function (Fig. 7c). The imaginary part of dielectric function of MoS_2 layers is larger than that of Au thin film thus leading to a larger electron energy loss; (iii) The resonance depth (i.e., the value of minimum reflectivity) is strongly dependent on the number of MoS_2 layers coated on the Au thin film (Fig. 7d). More specifically, the light energy absorbed by Au thin film is insufficient to promote a strong SPR excitation. The resonance depth of Au film with thickness less than 45 nm is much higher than that of the Au film with thickness greater than 45 nm. By further coating MoS_2 layers on the surface of Au film, the light absorption of the Au-MoS_2 structure can be effectively enhanced and thereby promoting a stronger SPR excitation (Fig. S1a). However, the enhancement effect of MoS_2 layers is overwhelmed by the electron energy loss when additional layers were coated on Au thin film with a thickness of 50 nm and above. The lowest value of minimum reflectivity (1.2680×10^{-8}) is obtained when the Au thickness is set at 45 nm and 3-layers of MoS_2 are used. As shown in Fig. 2b–5b, Fig. S1b-S12b and Supplementary Video 2, the Heaviside step-like phase jumps occur at the resonance angle where the resonance depth is the lowest at a fixed Au thin film thickness. For example, the sharpest phase changes for Au thin film with thicknesses of 46 nm and 48 nm are at the point of their respective lowest values of minimum reflectivity which are induced by the bilayer (blue curve in Fig. 3) and monolayer of MoS_2 (red curve in Fig. 4). Thus, 45 nm Au thin film and 3 layers of MoS_2 layers are the optimal parameters that need to be used to achieve the best sensitivity of the proposed SPR sensing system. Also, we have calculated that the sharpest phase signal change takes place with a resonance angle of 59.2592° (see Fig. 6).

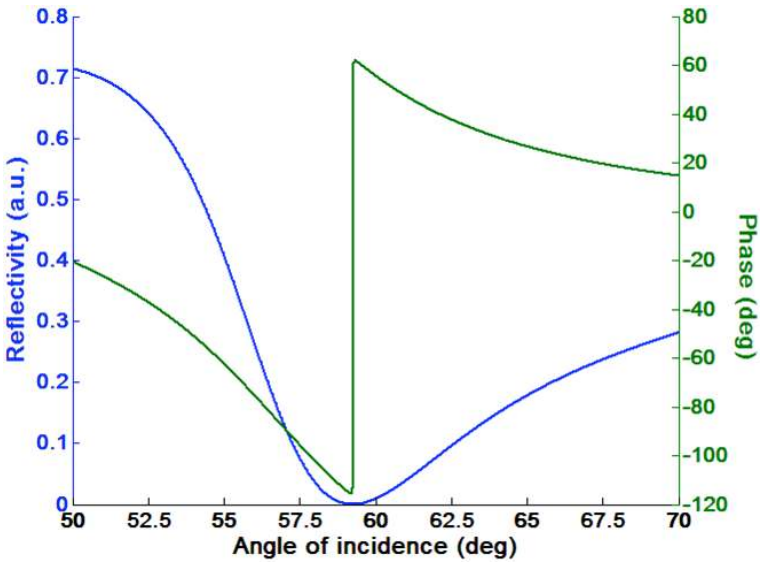

Fig. 6. Comparison of the reflectivity (blue) and phase (green) change as functions of the angle of light incidence with sensing layer refractive index 1.332 at wavelength 632.8 nm. The thickness of the gold layer is 45 nm and the number of MoS_2 layers is 3. Phase experiences a sharp singularity in the minimum of SPR curve.

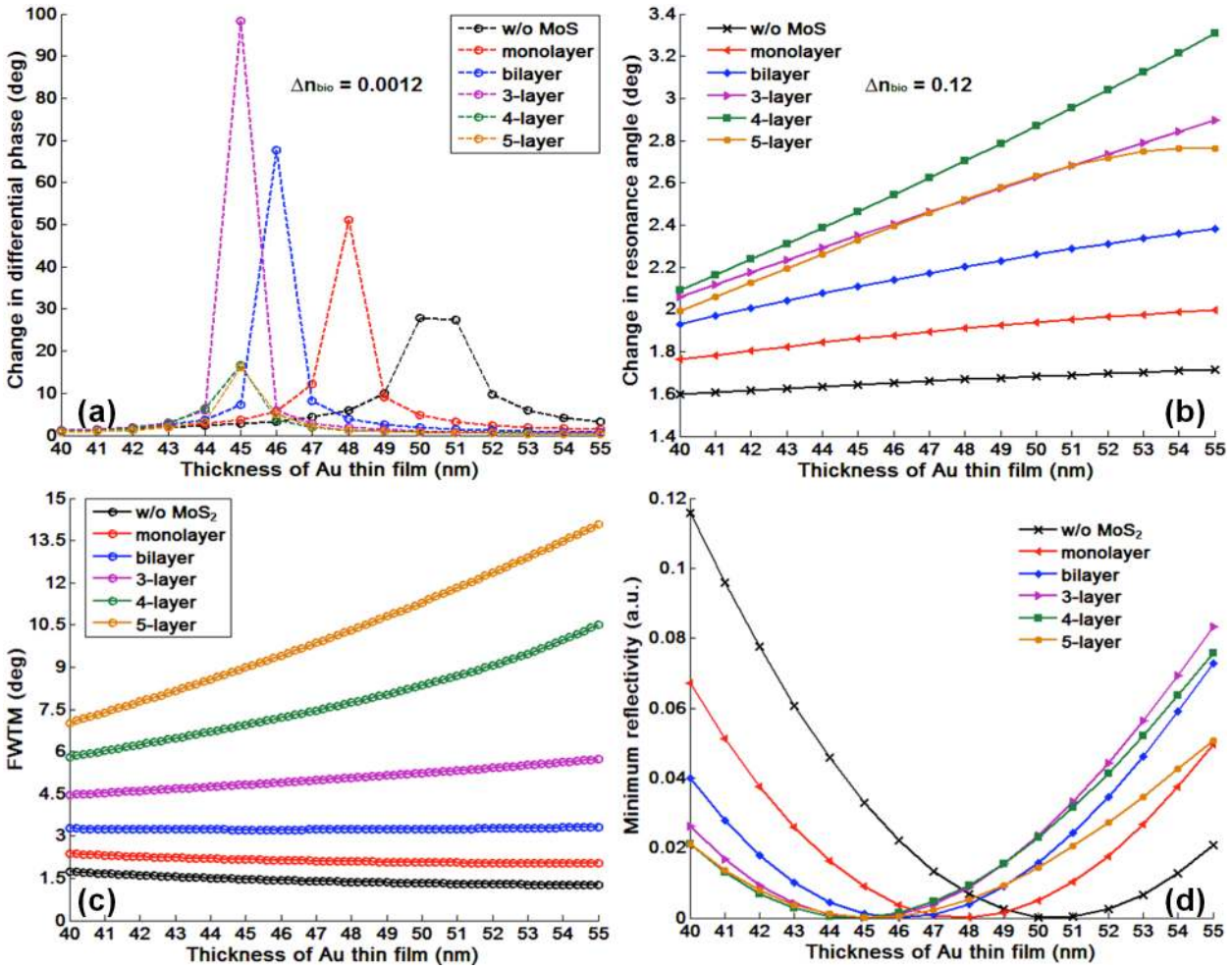

Fig. 7. Variation of change in (a) differential phase, (b) resonance angle due to the adsorption of biomolecules to the sensing surface, (c) FWTM and (d) minimum reflectivity in SPR curve with sensing layer refractive index 1.332, for various thicknesses of gold and different layers of MoS_2 at wavelength 632.8 nm. The symbols correspond to the values obtained from the simulated results while the continuous lines are the best-fit curves through these symbols.

To compare the phase and angular sensing performance of the graphene-MoS_2 structure based SPR biosensor, we plotted out the differential phase change ($\Delta\phi_d$) and resonance angle change ($\Delta\theta_{SPR}$) at a fixed refractive-index change ($\Delta n_{bio} = 0.0012$ or $\Delta n_{bio} = 0.12$) that is induced by the target molecular binding at the sensing surface as illustrated in Fig. 7a and 7b. The results showed that the resonance angle change ($\Delta\theta_{SPR}$) with a fixed Δn_{bio} is independent of the minimum reflectivity of the SPR curves before the adsorption of biomolecules and it increases with the increasing number of MoS_2 layers from 0 to 4 and subsequently saturated at 5 layers due to the loss by over-absorption of MoS_2 against its enhancement effect. The largest resonance

angle change ($\Delta\theta_{SPR}$) is ~3.3° for a large refractive-index change of 0.12 and with 4-layers MoS_2 coated between the monolayer graphene and 55 nm Au thin film (green curve in Fig. 7b). In comparison to the angular signal variation, the differential phase changes ($\Delta\phi_d$) are much more significant for even a tiny refractive-index change of 0.0012. The optimized phase results are respectively 51.0989° for monolayer MoS_2 coated 48 nm Au thin film, 67.6725° for bilayer MoS_2 coated 46 nm Au thin film and 98.2226° for 3-layer MoS_2 coated 45 nm Au thin film. It is worth noting that the differential phase changes with graphene-MoS_2 coated Au thin films are all larger than that of the monolayer graphene coated Au thin film with an optimum thickness of 50 nm ($\Delta\phi_d$ = 27.8046°), which demonstrates that the graphene-MoS_2 hybrid structure has a much better enhancement effect than that of the graphene material alone. If only graphene layers are deposited on the metallic thin film, the SPR signal enhancement effect will be compromised by the increment of electron energy loss in the system (see Fig. S13 and S14). We have summarized the sensing configurations and performances for the largest five differential phase changes to Δn_{bio} = 0.0012 for all the combinations of the Au thickness ranging from 40 nm to 55 nm and the number of MoS_2 layers (0 to 5) in Table 1. The table also shows that the lower the value of the minimum reflectivity, the larger the differential phase change.

Table 1
Optimized values of thickness of gold and the number of MoS_2 layers with corresponding change in resonance angle $\Delta\theta_{SPR}$ and differential phase $\Delta\phi_d$.

Au thickness	Number of MoS_2 layers	θ_{SPR} w/o biomolecules	θ_{SPR} with biomolecules	$\Delta\theta_{SPR}$ (Δn_{bio}=0.12)	$\Delta\phi_d$ (Δn_{bio}=0.0012)	FWTM	Minimum reflectivity
45nm	5	64.6186°	66.9486°	2.3300°	16.3305°	8.9808°	3.1928×10^{-5}
45nm	4	61.7380°	64.2028°	2.4648°	16.7458°	6.9507°	7.6821×10^{-5}
45nm	3	59.2592°	61.6090°	2.3498°	98.2226°	4.8269°	1.2680×10^{-8}
46nm	2	57.3250°	59.4671°	2.1421°	67.6725°	3.2275°	1.9026×10^{-6}
48nm	1	55.7940°	57.7043°	1.9103°	51.0989°	2.0956°	2.7116×10^{-5}
50nm	0	54.5661°	56.2499°	1.6838°	27.8046°	1.3260°	2.6143×10^{-4}

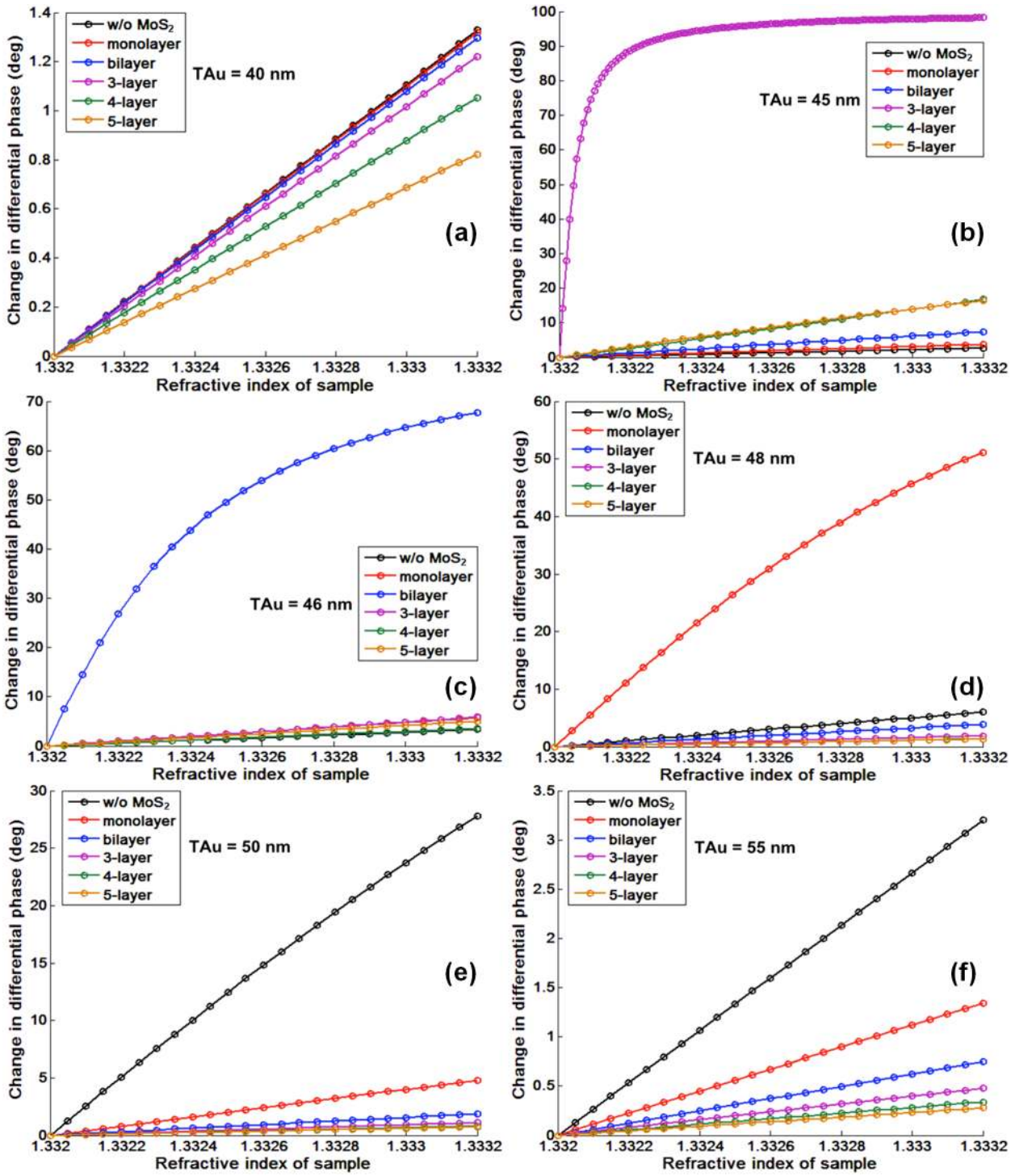

Fig. 8. Variation of change in differential phase with respect to sensing layer refractive index for different number of MoS_2 layers and a fixed thickness of gold layer: (a) 40 nm, (b) 45 nm, (c) 46 nm, (d) 48 nm, (e) 50 nm and (f) 55nm at wavelength 632.8 nm. The symbols correspond to the values obtained from the simulated results while the continuous lines are the best-fit curves through these symbols.

The phase signal changes to Δn_{bio} with different number of MoS_2 layers coated on Au thin film with thicknesses of 40 nm, 45 nm, 46 nm, 48 nm, 50 nm and 55 nm are shown in Fig. 8. The sensing signal for the configuration of 45 nm Au thin film coated with 3-layers MoS_2 and monolayer graphene exhibited a steep phase change from $\Delta n_{bio} = 1.332$ to $\Delta n_{bio} = 1.3322$ (purple curve in Fig. 8b), which shows great promise for detecting biomolecules with molecular weight less than 8 kDa or at concentration as low as 1 pM [22]. The incident angle for this sharp phase signal change is fixed at the SPR resonance angle of 59.2592°. If one wants to use this ultrasensitive configuration to detect a larger Δn_{bio}, one only needs to shift the incident angle ±0.001° away from the resonance angle for a linear phase signal change or to choose other combinations of Au thin film thickness and number of MoS_2 layers like bilayer MoS_2-coated 46 nm Au thin film (blue curve in Fig. 8c) or monolayer MoS_2-coated 48 nm Au thin film (red curve in Fig. 8d) for achieving the best detection sensitivity. To further confirm the strong SPR excitation of 3-layers MoS_2 coated between monolayer graphene and 45 nm Au thin film, we employed finite element analysis (FEA) method (COMSOL Multiphysics 4.3a) to study the electric field distribution inside the graphene-MoS_2 structure based sensing system at the resonance angle (see Fig. 9). It can be seen that a large electric field enhancement is generated at the sensing surface and the probing field intensity exponentially decayed to the sensing medium that contains the target biomolecules with a penetration depth around 150 nm. The penetration depth is defined as the distance where the electric field is reduced to 1/e of its value. Thus, the electric probing field close to the graphene capture layer is very intense and highly sensitive to small biomolecule interactions. According to Eq. (16) and Eq. (17), the SPR phase sensitivity is proportional to the differential phase change ($\Delta\phi_d$) for a fixed Δn_{bio} and therefore the enhancement factor for the graphene-MoS_2 enhanced SPR biosensor is determined by the ratio of their differential phase change ($\Delta\phi_{dmmg}/\Delta\phi_{dm}$) for the same refractive index change that is induced by the target molecule bindings. The linear phase signal changes detected by the conventional SPR sensor with pure Au thin film, graphene-based SPR biosensor and graphene-MoS_2 based SPR biosensor for a tiny refractive-index change (Δn_{bio}) as low as 10^{-6} RIU are plotted in Fig. 10. The enhancement factor (E_p) for the graphene-MoS_2 based SPR biosensor is calculated to have more than 500-fold of increment when compared to both the conventional and graphene based SPR sensors with the same thickness of Au thin film.

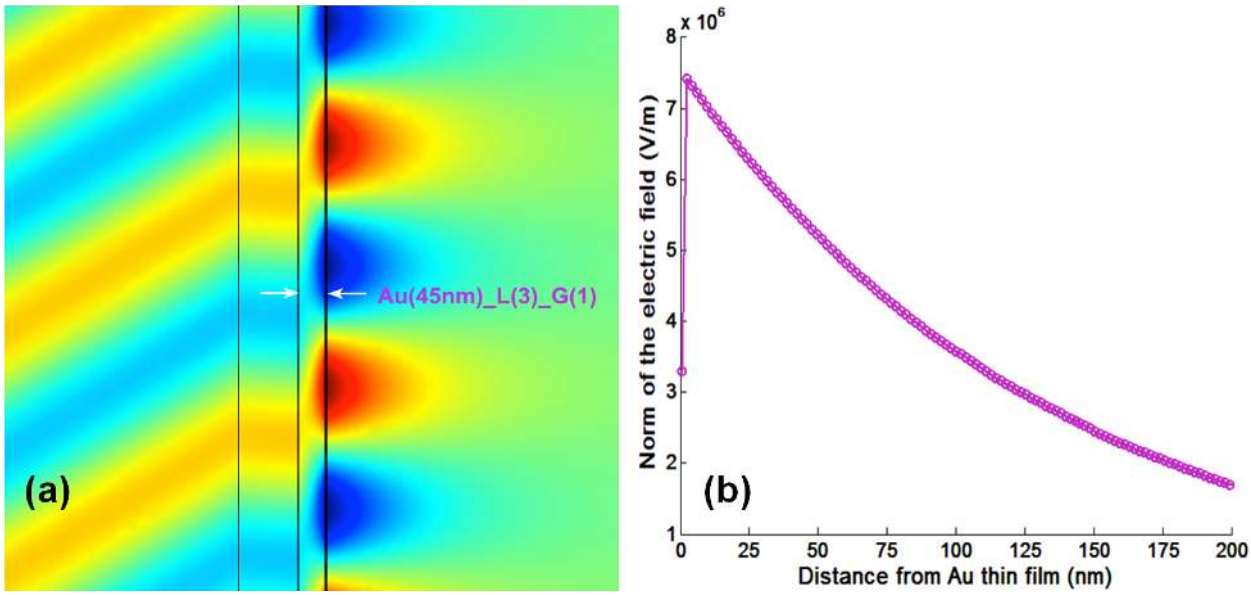

Fig. 9. FEA simulations of resonant graphene–MoS_2 enhanced Au sensing film. (a) Electric field distribution at the SPR resonance angle 59.2592°. (b) Cross-section plot of the total electric field along the direction perpendicular to the prism base, showing clear evanescent field at the sensing interface.

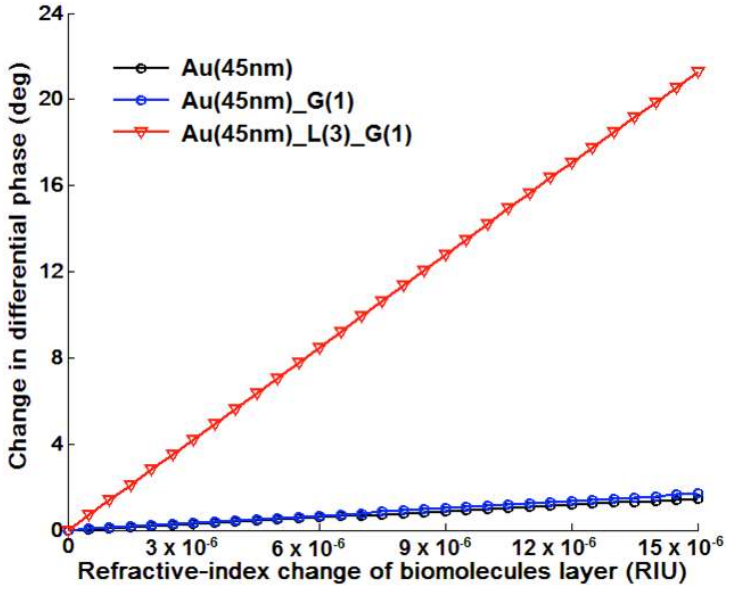

Fig. 10. Comparison of the SPR sensing performances with pure Au thin film, monolayer graphene coated Au thin film and monolayer graphene-MoS_2 coated Au thin film (3 layers of MoS_2) for a tiny refractive-index change (as low as 10^{-6} RIU) due to adsorption of biomolecules on the sensing surface. The differential phase signals for pure Au thin film and monolayer graphene coated Au thin film (black and blue curves) are magnified by a factor of 50 for clarity.

4. Conclusions

In this study, a highly sensitive graphene-MoS_2 nanobiosensor based on differential phase measurement is presented. The sensing substrate consists of MoS_2 and graphene deposited Au thin film. Monolayer graphene acts as a bio-recognition component to selectively detect targeting biomolecules through pi-stacking force. In addition, our theoretical analysis shows that electron transfer due to the work functions difference between graphene, MoS_2 and Au will result in a large electric field enhancement at the sensing interface and thus leading to an ultrahigh sensitivity of the sensing system. Since monolayer MoS_2 had a higher light absorption rate than that of graphene, a stronger SPR excitation can be achieved by using the graphene-MoS_2 hybrid structure as the sensing substrate. In comparison to angular measurement that requires a large number of MoS_2 (5 to 10) to improve the sensitivity of the SPR system, phase detection only depends on the minimum reflectivity of the sensing system which allows one to use a fewer number of MoS_2 layers and an enhancement factor of more than 2 orders is demonstrated by using 3-layers MoS_2 and a monolayer graphene coated on the 45 nm Au thin film. Also, we have found that the width of the SPR reflectivity curves can be significantly reduced by using a fewer number of MoS_2 layers together with the phase interrogation detection method and this will provide higher detection accuracy for the system.

References:

[1] A.K. Geim and I.V. Grigorieva, "Van der Waals heterostructures," *Nature*, vol. 499, pp. 419-425, 2013.

[2] S. Zeng, D. Baillargeat, H.-P. Ho, and K.-T. Yong, "Nanomaterials enhanced surface plasmon resonance for biological and chemical sensing applications," *Chemical Society Reviews*, vol. 43, pp. 3426-3452, 2014.

[3] M. Xu, T. Liang, M. Shi, and H. Chen, "Graphene-like two-dimensional materials," *Chemical Reviews*, vol. 113, pp. 3766-3798, 2013.

[4] Q.H. Wang, K. Kalantar-Zadeh, A. Kis, J.N. Coleman, and M.S. Strano, "Electronics and optoelectronics of two-dimensional transition metal dichalcogenides," *Nature Nanotechnology*, vol. 7, pp. 699-712, 2012.

[5] M. Chhowalla, H.S. Shin, G. Eda, L.-J. Li, K.P. Loh, and H. Zhang, "The chemistry of two-dimensional layered transition metal dichalcogenide nanosheets," *Nature Chemistry*, vol. 5, pp. 263-275, 2013.

[6] G. Eda and S.A. Maier, "Two-dimensional crystals: managing light for optoelectronics," *Acs Nano*, vol. 7, pp. 5660-5665, 2013.

[7] K.S. Novoselov and A.H.C. Neto, "Two-dimensional crystals-based heterostructures: materials with tailored properties," *Physica Scripta*, vol. T146, 014006. 2012.

[8] L. Yu, Y.-H. Lee, X. Ling, E.J.G. Santos, Y.C. Shin, Y. Lin, M. Dubey, E. Kaxiras, J. Kong, H. Wang, and T. Palacios, "Graphene/MoS_2 hybrid technology for large-scale two-dimensional electronics," *Nano Letters*, vol. 14, pp. 3055-3063, 2014.

[9] K.V. Sreekanth, S. Zeng, J.Z. Shang, K.T. Yong, and T. Yu, "Excitation of surface electromagnetic waves in a graphene-based Bragg grating," *Scientific Reports*, vol. 2, 737. 2012.

[10] J. Xia, X. Huang, L.-Z. Liu, M. Wang, L. Wang, B. Huang, D.-D. Zhu, J.-J. Li, C.-Z. Gu, and X.-M. Meng, "CVD synthesis of large-area, highly crystalline $MoSe_2$ atomic layers on diverse substrates and application to photodetectors," *Nanoscale*, vol. 6, pp. 8949-8955, 2014.

[11] K.S. Novoselov, A.K. Geim, S.V. Morozov, D. Jiang, Y. Zhang, S.V. Dubonos, I.V. Grigorieva, and A.A. Firsov, "Electric field effect in atomically thin carbon films," *Science*, vol. 306, pp. 666-669, 2004.

[12] D.C. Elias, R.V. Gorbachev, A.S. Mayorov, S.V. Morozov, A.A. Zhukov, P. Blake, L.A. Ponomarenko, I.V. Grigorieva, K.S. Novoselov, F. Guinea, and A.K. Geim, "Dirac cones reshaped by interaction effects in suspended graphene," *Nature Physics*, vol. 7, pp. 701-704, 2011.

[13] A. Hoggard, L.-Y. Wang, L. Ma, Y. Fang, G. You, J. Olson, Z. Liu, W.-S. Chang, P.M. Ajayan, and S. Link, "Using the plasmon linewidth to calculate the time and efficiency of electron transfer between gold nanorods and graphene," *Acs Nano*, vol. 7, pp. 11209-11217, 2013.

[14] J. Kim, H. Son, D.J. Cho, B. Geng, W. Regan, S. Shi, K. Kim, A. Zettl, Y.-R. Shen, and F. Wang, "Electrical control of optical plasmon resonance with graphene," *Nano Letters*, vol. 12, pp. 5598-5602, 2012.

[15] J. Niu, Y.J. Shin, Y. Lee, J.-H. Ahn, and H. Yang, "Graphene induced tunability of the surface plasmon resonance," *Applied Physics Letters*, vol. 100, 061116. 2012.

[16] S. Lee, M.H. Lee, H.-j. Shin, and D. Choi, "Control of density and LSPR of Au nanoparticles on graphene," *Nanotechnology*, vol. 24, 275702. 2013.

[17] N. Reckinger, A. Vlad, S. Melinte, J.-F. Colomer, and M. Sarrazin, "Graphene-coated holey metal films: tunable molecular sensing by surface plasmon resonance," *Applied Physics Letters*, vol. 102, 211108. 2013.

[18] A.M. Zaniewski, M. Schriver, J.G. Lee, M.F. Crommie, and A. Zettl, "Electronic and optical properties of metal-nanoparticle filled graphene sandwiches," *Applied Physics Letters*, vol. 102, 023108. 2013.

[19] S. Zeng, K.-T. Yong, I. Roy, X.-Q. Dinh, X. Yu, and F. Luan, "A review on functionalized gold nanoparticles for biosensing applications," *Plasmonics*, vol. 6, pp. 491-506, 2011.

[20] S. Zeng, X. Yu, W.-C. Law, Y. Zhang, R. Hu, X.-Q. Dinh, H.-P. Ho, and K.-T. Yong, "Size dependence of Au NP-enhanced surface plasmon resonance based on differential phase measurement," *Sensors and Actuators B-Chemical*, vol. 176, pp. 1128-1133, 2013.

[21] E. Wijaya, C. Lenaerts, S. Maricot, J. Hastanin, S. Habraken, J.-P. Vilcot, R. Boukherroub, and S. Szunerits, "Surface plasmon resonance-based biosensors: from the development of different SPR structures to novel surface functionalization strategies," *Current Opinion in Solid State & Materials Science*, vol. 15, pp. 208-224, 2011.

[22] L. Wu, H.S. Chu, W.S. Koh, and E.P. Li, "Highly sensitive graphene biosensors based on surface plasmon resonance," *Optics Express*, vol. 18, pp. 14395-14400, 2010.

[23] B. Song, D. Li, W.P. Qi, M. Elstner, C.H. Fan, and H.P. Fang, "Graphene on Au(111): a highly conductive material with excellent adsorption properties for high-resolution bio/nanodetection and identification," *Chemphyschem*, vol. 11, pp. 585-589, 2010.

[24] G.B. McGaughey, M. Gagne, and A.K. Rappe, "Pi-stacking interactions - alive and well in proteins," *Journal of Biological Chemistry*, vol. 273, pp. 15458-15463, 1998.

[25] S.H. Choi, Y.L. Kim, and K.M. Byun, "Graphene-on-silver substrates for sensitive surface plasmon resonance imaging biosensors," *Optics Express*, vol. 19, pp. 458-466, 2011.

[26] R. Verma, B.D. Gupta, and R. Jha, "Sensitivity enhancement of a surface plasmon resonance based biomolecules sensor using graphene and silicon layers," *Sensors and Actuators B-Chemical*, vol. 160, pp. 623-631, 2011.

[27] P.K. Maharana and R. Jha, "Chalcogenide prism and graphene multilayer based surface plasmon resonance affinity biosensor for high performance," *Sensors and Actuators B-Chemical*, vol. 169, pp. 161-166, 2012.

[28] H. Zhang, Y. Sun, S. Gao, J. Zhang, H. Zhang, and D. Song, "Novel graphene oxide-based surface plasmon resonance biosensor for immunoassay," *Small*, vol. 9, pp. 2537-2540, 2013.

[29] R.R. Nair, P. Blake, A.N. Grigorenko, K.S. Novoselov, T.J. Booth, T. Stauber, N.M.R. Peres, and A.K. Geim, "Fine structure constant defines visual transparency of graphene," *Science*, vol. 320, pp. 1308-1308, 2008.

[30] O. Salihoglu, S. Balci, and C. Kocabas, "Plasmon-polaritons on graphene-metal surface and their use in biosensors," *Applied Physics Letters*, vol. 100, 213110. 2012.

[31] K. Roy, M. Padmanabhan, S. Goswami, T.P. Sai, G. Ramalingam, S. Raghavan, and A. Ghosh, "Graphene-MoS_2 hybrid structures for multifunctional photoresponsive memory devices," *Nature Nanotechnology*, vol. 8, pp. 826-830, 2013.

[32] P.T.K. Loan, W. Zhang, C.-T. Lin, K.-H. Wei, L.-J. Li, and C.-H. Chen, "Graphene/MoS_2 heterostructures for ultrasensitive detection of DNA hybridisation," *Advanced Materials*, vol. 26, pp. 4838–4844, 2014.

[33] S. Bertolazzi, D. Krasnozhon, and A. Kis, "Nonvolatile memory cells based on MoS_2/graphene heterostructures," *Acs Nano*, vol. 7, pp. 3246-3252, 2013.

[34] O. Lopez-Sanchez, D. Lembke, M. Kayci, A. Radenovic, and A. Kis, "Ultrasensitive photodetectors based on monolayer MoS_2," *Nature Nanotechnology*, vol. 8, pp. 497-501, 2013.

[35] B. Radisavljevic, A. Radenovic, J. Brivio, V. Giacometti, and A. Kis, "Single-layer MoS_2 transistors," *Nature Nanotechnology*, vol. 6, pp. 147-150, 2011.

[36] K.F. Mak, C. Lee, J. Hone, J. Shan, and T.F. Heinz, "Atomically thin MoS_2: a new direct-gap semiconductor," *Physical Review Letters*, vol. 105, 136805. 2010.

[37] D.-S. Tsai, K.-K. Liu, D.-H. Lien, M.-L. Tsai, C.-F. Kang, C.-A. Lin, L.-J. Li, and J.-H. He, "Few-layer MoS_2 with high broadband photogain and fast optical switching for use in harsh environments," *Acs Nano*, vol. 7, pp. 3905-3911, 2013.

[38] W. Zhang, C.-P. Chuu, J.-K. Huang, C.-H. Chen, M.-L. Tsai, Y.-H. Chang, C.-T. Liang, Y.-Z. Chen, Y.-L. Chueh, J.-H. He, M.-Y. Chou, and L.-J. Li, "Ultrahigh-gain photodetectors based on atomically thin graphene-MoS_2 heterostructures," *Scientific Reports*, vol. 4, 3826. 2014.

[39] G. Giovannetti, P.A. Khomyakov, G. Brocks, V.M. Karpan, J. van den Brink, and P.J. Kelly, "Doping graphene with metal contacts," *Physical Review Letters*, vol. 101, 026803. 2008.

[40] B. Sachs, L. Britnell, T.O. Wehling, A. Eckmann, R. Jalil, B.D. Belle, A.I. Lichtenstein, M.I. Katsnelson, and K.S. Novoselov, "Doping mechanisms in graphene-MoS_2 hybrids," *Applied Physics Letters*, vol. 103, 251607. 2013.

[41] L. Britnell, R.M. Ribeiro, A. Eckmann, R. Jalil, B.D. Belle, A. Mishchenko, Y.J. Kim, R.V. Gorbachev, T. Georgiou, S.V. Morozov, A.N. Grigorenko, A.K. Geim, C. Casiraghi, A.H.C. Neto, and K.S. Novoselov, "Strong light-matter interactions in heterostructures of atomically thin films," *Science*, vol. 340, pp. 1311-1314, 2013.

[42] X.S. Li, Y.W. Zhu, W.W. Cai, M. Borysiak, B.Y. Han, D. Chen, R.D. Piner, L. Colombo, and R.S. Ruoff, "Transfer of large-area graphene films for high-performance transparent conductive electrodes," *Nano Letters*, vol. 9, pp. 4359-4363, 2009.

[43] Y.Y. Hui, X. Liu, W. Jie, N.Y. Chan, J. Hao, Y.-T. Hsu, L.-J. Li, W. Guo, and S.P. Lau, "Exceptional tunability of band energy in a compressively strained trilayer MoS_2 sheet," *Acs Nano*, vol. 7, pp. 7126-7131, 2013.

[44] M.N. Polyanskiy, "Refractive index database," http://refractiveindex.info.

[45] E.D. Palik, *Handbook of optical constants of solids*, New York: Academic, 1985.

[46] B.D. Gupta and A.K. Sharma, "Sensitivity evaluation of a multi-layered surface plasmon resonance-based fiber optic sensor: a theoretical study," *Sensors and Actuators B-Chemical*, vol. 107, pp. 40-46, 2005.

[47] H. Raether, *Surface plasmons on smooth and rough surfaces and on gratings*, Berlin: Springer-Verlag, 1988.

[48] A. Castellanos-Gomez, N. Agrait, and G. Rubio-Bollinger, "Optical identification of atomically thin dichalcogenide crystals," *Applied Physics Letters*, vol. 96, 213116. 2010.

[49] M. Bruna and S. Borini, "Optical constants of graphene layers in the visible range," *Applied Physics Letters*, vol. 94, 031901. 2009.

[50] M. Daimon and A. Masumura, "Measurement of the refractive index of distilled water from the near-infrared region to the ultraviolet region," *Applied Optics*, vol. 46, pp. 3811-3820, 2007.

[51] K.V. Sreekanth, K.H. Krishna, A. De Luca, and G. Strangi, "Large spontaneous emission rate enhancement in grating coupled hyperbolic metamaterials," *Scientific Reports*, vol. 4, 6340. 2014.

[52] K.V. Sreekanth, S. Zeng, K.-T. Yong, and T. Yu, "Sensitivity enhanced biosensor using graphene-based one-dimensional photonic crystal," *Sensors and Actuators B-Chemical*, vol. 182, pp. 424-428, 2013.

[53] V.G. Kravets, F. Schedin, R. Jalil, L. Britnell, R.V. Gorbachev, D. Ansell, B. Thackray, K.S. Novoselov, A.K. Geim, A.V. Kabashin, and A.N. Grigorenko, "Singular phase nano-optics in plasmonic metamaterials for label-free single-molecule detection," *Nature Materials*, vol. 12, pp. 304-309, 2013.

[54] A.V. Kabashin, S. Patskovsky, and A.N. Grigorenko, "Phase and amplitude sensitivities in surface plasmon resonance bio and chemical sensing," *Optics Express*, vol. 17, pp. 21191-21204, 2009.

[55] I. Pockrand, "Surface plasma oscillations at silver surfaces with thin transparent and absorbing coatings," *Surface Science*, vol. 72, pp. 577-588, 1978.

Supporting Video1: https://www.researchgate.net/publication/277666937_Supporting_video_1,

Supporting Video2: https://www.researchgate.net/publication/277666946_Supporting_video_2.